ADVANCED SCIENCE
Open Access

Supporting Information

for *Adv. Sci.*, DOI 10.1002/advs.202104835

Monitoring Wound Healing with Topically Applied Optical NanoFlare mRNA Nanosensors

Jangsun Hwang, Youngmin Seo, Daun Jeong, Xiaoyu Ning, Christian Wiraja, Lixia Yang, Chew Teng Tan, Jinhyuck Lee, Yesol Kim, Ji Won Kim, Dai Hyun Kim, Jonghoon Choi, Chin Yan Lim, Kanyi Pu, Woo Young Jang and Chenjie Xu**

Supplementary information for

Monitoring wound healing with topically applied optical NanoFlare mRNA nanosensors

Jangsun Hwang[1,2], Youngmin Seo[3,4], Daun Jeong[2], Xiaoyu Ning[1,5], Christian Wiraja[1], Lixia Yang[1], Chew Teng Tan[6], Jinhyuck Lee[2], Yesol Kim[7], Ji Won Kim[7], Dai Hyun Kim[8], Jonghoon Choi[7], Chin Yan Lim[6,9], Kanyi Pu[1], Woo Young Jang[2*], Chenjie Xu[10*]

[1] School of Chemical and Biomedical Engineering, Nanyang Technological University, 62 Nanyang Drive, Singapore, 637457

[2] Department of Orthopedic Surgery, College of Medicine, Korea University, 73 Korea-ro, Seongbuk-gu, Seoul, Republic of Korea, 02841

[3] School of Electrical and Electronic Engineering, Yonsei University, 50 Yonsei-ro, Seodaemun-gu, Seoul, Republic of Korea, 03722

[4] Department of Research & Development, OID Ltd, 249-2, 123 Osongsaengmyeong-ro, Osong-eup, Heungdeok-gu, Cheongju-si, Chungcheongbuk-do, Republic of Korea, 28160

[5] NTU Institute for Health Technologies, Interdisciplinary Graduate School, Nanyang Technological University, 61 Nanyang Drive, Singapore, 637335

[6] A*STAR Skin Research Labs, Agency for Science, Technology and Research, 8A Biomedical Grove, Singapore 138648

[7] School of Integrative Engineering, Chung-Ang University, 84, Heukseok-ro, Dongjak-gu, Seoul, Republic of Korea, 06974

[8] Department of Dermatology, College of Medicine, Korea University, 73 Korea-ro, Seongbuk-gu , Seoul, Republic of Korea, 02841

[9] Department of Biochemistry, Yong Loo Lin School of Medicine, National University of Singapore, MD 7, 8 Medical Drive, Singapore 117596

[10] Department of Biomedical Engineering, City University of Hong Kong, 83 Tat Chee Avenue, Kowloon, Hong Kong SAR, China

[*] Correspondence to chenjie.xu@cityu.edu.hk and opmanse@korea.ac.kr

Flare	−ΔG(Duplex) (kcal/mol)*	
	FSP1 (human)	FSP1 (mouse)
12 nt	13.7	
14 nt	16.9	
15 nt	18.7	21.4
16 nt	21.0	
18 nt	24.5	
Target	53.4	58.6
	PECAM1 (human)	PECAM1 (mouse)
15 nt	19.4	21.4
Target	48.9	61.4
	KRT14 (human)	KRT14 (mouse)
15 nt	20.8	20.8
Target	56.8	56.8
	GAPDH (human)	GAPDH (mouse)
15 nt	19.6	20.9
Target	57.8	59.9
*Predicted using RNA Structure		

Table S1. The predicted free energy change of the R-F (recognition-flare) duplex with varied flare length of 12, 14, 15, 16, and 18 nt (human and mouse).

Binding free energy of Nanoflare	R+T	R+F	RF/FT (%)	GC contents (%)	Recovery kinetics , Saturation
	−ΔG(Duplex) (kcal/mol)				
FSP1	53.4	18.7	35	46	(high, fast)
KRT14	56.8	20.8	36.6	53	(low, slow)
PECAM1	48.9	19.4	39.7	46	(low, fast)
GAPDH	57.8	19.6	33.9	53	(high, slow)

Table S2. Recovery kinetics and saturation time of NFs

Protein	Gene	Forward	Reverse
FSP-1	S100A4	5'-TGAGCAACTTGGACAGCAACA-3'	5'-ATTTCTTCCTGGGCTGCTTATCT-3'
CTGF	CCN2	CAGCATGGACGTTCGTCTG	AACCACGGTTTGGTCCTTGG
Collagen-1	COL1A1	TCTGCGACAACGGCAAGGTG	GACGCCGGTGGTTTCTTGGT
HSP47	SERPINH1	AACCGTGGCTTCATGGTGACTC	TGATGAGGCTGGAGAGCTTGTG
α-SMA	ACTA2	CTATGCCTCTGGACGCACAACT	CAGATCCAGACGCATGATGGCA
CD24	CD24	CACGCAGATTTATTCCAGTGAAAC	GACCACGAAGAGACTGGCTGTT
CD26	DPP4	AAAGGCACCTGGGAAGTCATCG	CAGCTCACAACTGAGGCATGTC
CD90	THY1	GAAGGTCCTCTACTTATCCGCC	TGATGCCCTCACACTTGACCAG
SCA-1	ATXN1	AGATCGACTCCAGCACCGTAGA	CTCTACCAAAACTTCAACGCTGAC
DDR2	DDR2	AACGAGAGTGCCACCAATGGCT	ACTCACTGGCTTCAGAGCGGAA
MMP-2	MMP2	AGCGAGTGGATGCCGCCTTTAA	CATTCCAGGCATCTGCGATGAG
Vimentin	VIM	AGGCAAAGCAGGAGTCCACTGA	ATCTGGCGTTCCAGGGACTCAT
Protein	**Gene**	**Forward**	**Reverse**
Keratin 10	KRT10	5'-CCTGCTTCAGATCGACAATGCC-3'	5'-ATCTCCAGGTCAGCCTTGGTCA-3'
Keratin 14	KRT14	TGCCGAGGAATGGTTCTTCACC	GCAGCTCAATCTCCAGGTTCTG
Keratin 1	KRT1	CAGCATCATTGCTGAGGTCAAGG	CATGTCTGCCAGCAGTGATCTG
Keratin 5	KRT5	GCTGCCTACATGAACAAGGTGG	ATGGAGAGGACCACTGAGGTGT
Keratin 16	KRT16	CTACCTGAGGAAGAACCACGAG	CTCGTACTGGTCACGCATCTCA
Involucrin	IVL	GGTCCAAGACATTCAACCAGCC	TCTGGACACTGCGGGTGGTTAT
Filaggrin	FLG	GCTGAAGGAACTTCTGGAAAAGG	GTTGTGGTCTATATCCAAGTGATC
Transglutaminase	TGM1	GAACGACTGCTGGATGAAGAGG	CTTGATGGACTCCACAGAGCAG
P2X purinoceptor 7	P2RX7	CGACTAGGAGACATCTTCCGAG	GCAGTGATGGAACCAACGGTCT
P2Y purinoceptor 2	P2RY2	CGAGGACTTCAAGTACGTGCTG	GTGGACGCATTCCAGGTCTTGA
Caspase 14	CASP14	GGTGGATGTGTTCACGAAGAGG	CCTTCTTGAACCAGCTCTGCTTC
SPRR2A	SPRR2A	CAGTGCCAGCAGAAATATCCT	CCAAATATCCTTATCCTTTCTTGG
Protein	**Gene**	**Forward**	**Reverse**
PECAM-1/CD31	PECAM1	5'-AAGTGGAGTCCAGCCGCATATC-3'	5'-ATGGAGCAGGACAGGTTCAGTC-3'
KDR/VEGFR2	KDR	GGAACCTCACTATCCGCAGAGT	CCAAGTTCGTCTTTTCCTGGGC
VEGFR1	FLT1	CCTGCAAGATTCAGGCACCTATG	TTGCAGTGCTCACCTCTGATT
CD34	CD34	CCTCAGTGTCTACTGCTGGTCT	GGAATAGCTCTGGTGGCTTGCA
Endoglin/CD105	ENG	CGGTGGTCAATATCCTGTCGAG	AGGAAGTGTGGGCTGAGGTAGA
MCAM/CD146	MCAM	ATCGCTGCTGAGTGAACCACAG	CTACTCTCTGCCTCACAGGTCA
ICAM-1	ICAM1	AGCGGCTGACGTGTGCAGTAAT	TCTGAGACCTCTGGCTTCGTCA
VCAM-1	VCAM1	GATTCTGTGCCCACAGTAAGGC	TGGTCACAGAGCCACCTTCTTG
VE-Cadherin /CD144	CDH5	GAAGCCTCTGATTGGCACAGTG	TTTTGTGACTCGGAAGAACTGGC
vWF	VWF	CCTTGAATCCCAGTGACCCTGA	GGTTCCGAGATGTCCTCCACAT
Tie-2	TEK	GGTCAAGCAACCCAGCCTTTTC	CAGGTCATTCCAGCAGAGCCAA
EDG1/S1PR1	S1PR1	CCTGTGACATCCTCTTCAGAGC	CACTTGCAGCAGGACATGATCC

Table S3. Primer information.

Gene	Nucleotide		Sequence
FSP1	Human Recognition Mouse Recognition		5′- ATTTCTTCCTGGGCTGCTTATCTGGGAAAAAAAA-SH 3′ 5′- ACTTCTTCCGGGGCTCCTTATCTGGGCAAAAAAA-SH 3
	Flare		
	Length	Human 18 nt	3′- CCCGACGAATAGACCCTT- **FAM** -5′
		Human 16 nt	3′- CGACGAATAGACCCTT- **FAM** -5′
		Human 15 nt	3′- GACGAATAGACCCTT- **FAM** -5′
		Mouse 15 nt	3′- GAGGAATAGACCCGT- **Cy3** -5′
		Human 14 nt	3′- ACGAATAGACCCTT- **FAM** -5′
		Human 12nt	3′- GAATAGACCCTT- **FAM** -5′
PECAM1	Human Recognition Mouse Recognition		5'-ATGGAGCAGGACAGGTTCAGTCTTTCAC AAAAAA-SH-3' 5'-TTAAGGGAGCCTTCCGTTCTTAGGGTCGACAAAAAA-SH-3'
	Human Flare Mouse Flare		3'-CCAAGTCAGAAAGTG-**Cy3**-5' 3'-CAAGAATCCCAGCTG-**Cy3**-5'
KRT14	Human Recognition Same as human		5′- GACTGCAGCTCAATCTCCAGGTTCTGCAAAAAAA-SH -3′
	Human Flare Same as human		3′- AGAGGTCCAAGACGT- **Cy3** -5′
GAPDH	Human Recognition Mouse Recognition		5′- GATGGCATGGACTGTGGTCATGAGTCCTAAAAAA-3′ 5′- GATGGCATGGACTGTGGTCATGAGCCCTAAAAAA-3′
	Human Flare Mouse Flare		3'-CACCAGTACTCAGGA-**Cy5**-5' 3'-CACCAGTACTCGGGA-**Cy5**-5'

Table S4. Sequence of recognitions and flares for NanoFlare.

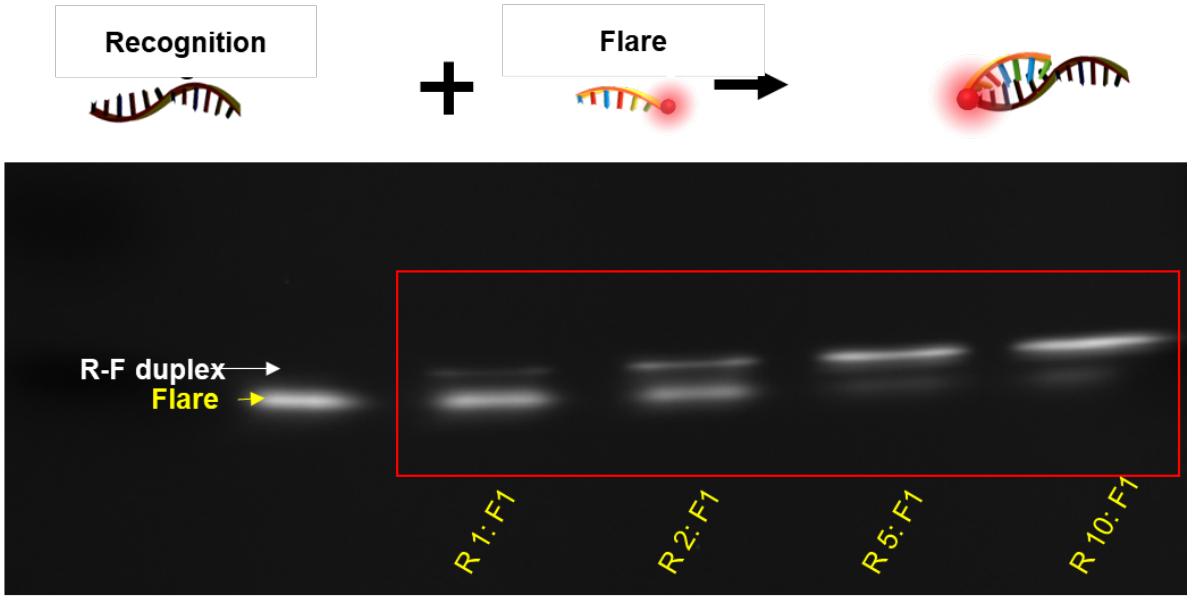

Supplementary Figure S1. Optimization of R:F ratio for the R-F duplex hybridization. Polyacrylamide gel electrophoresis of R-F hybridization under different R:F ratios (R and F concentration: 100 μM, R: F=v/v).

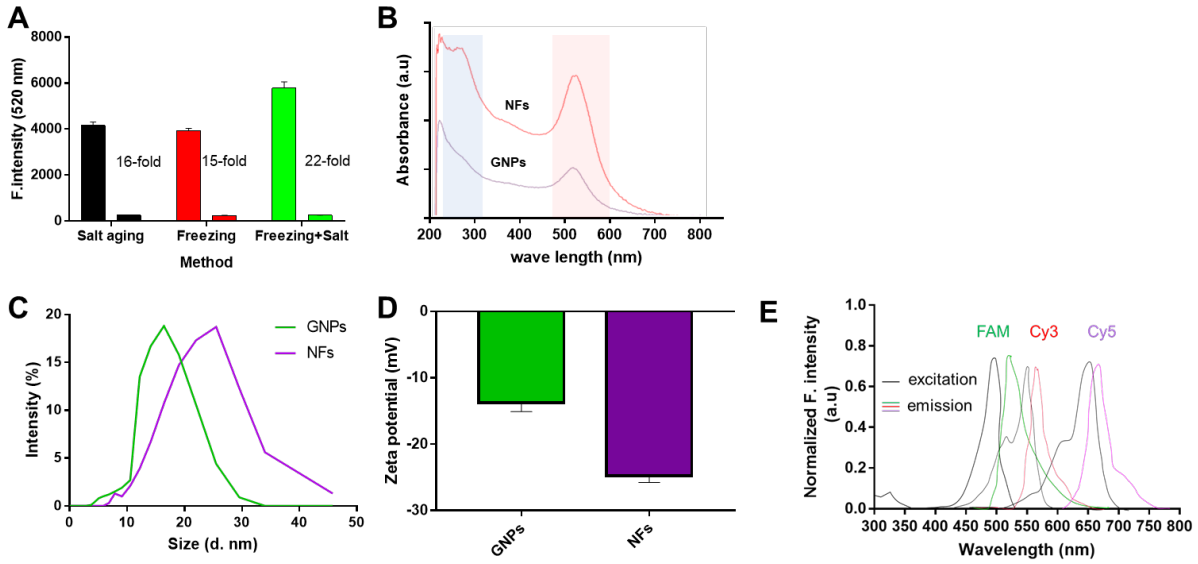

Supplementary Figure S2. Characterization of NanoFlares (NFs): (A) The change of fluorescence signal upon the mixing of target sequence and NFs made from different methods; **(B)** Absorbance spectra of gold nanoparticles (GNPs) and NF; **(C)** Hydrodynamic diameters; **(D)** Zeta-potentials of GNPs and NFs (n=3, values are means ± s.d.); **(E)** Excitation and emission spectra of FAM (493-517 nm), Cy3 (555-569 nm), and Cy5 (651-670 nm).

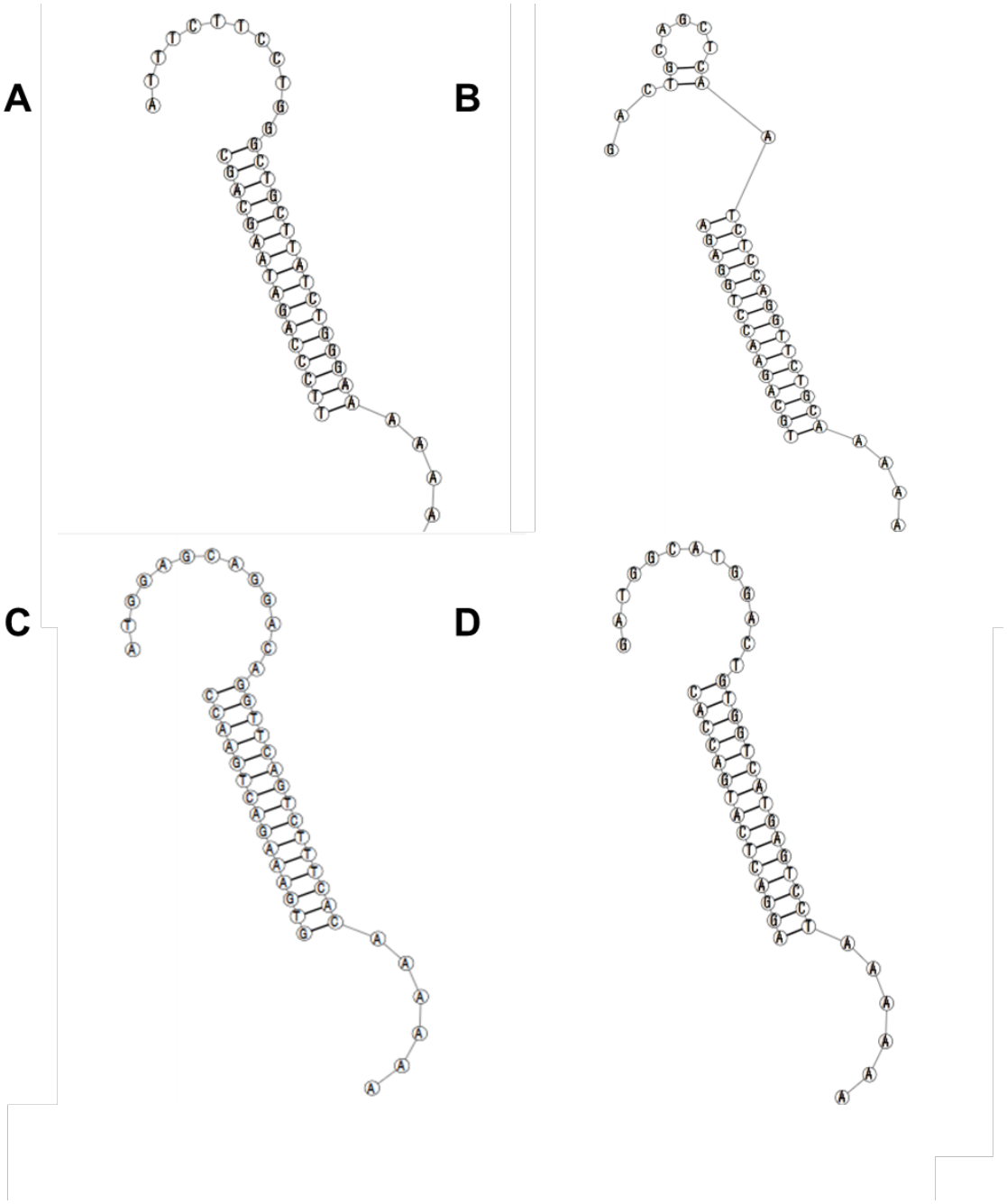

Supplementary Figure S3. R+F selection: (A) Possible secondary structure prediction of the R-F (recognition-flare) duplex for FSP1-NFs; **(B)** KRT14-NFs; **(C)** PECAM1-NFs; **(D)** GAPDH-NFs.

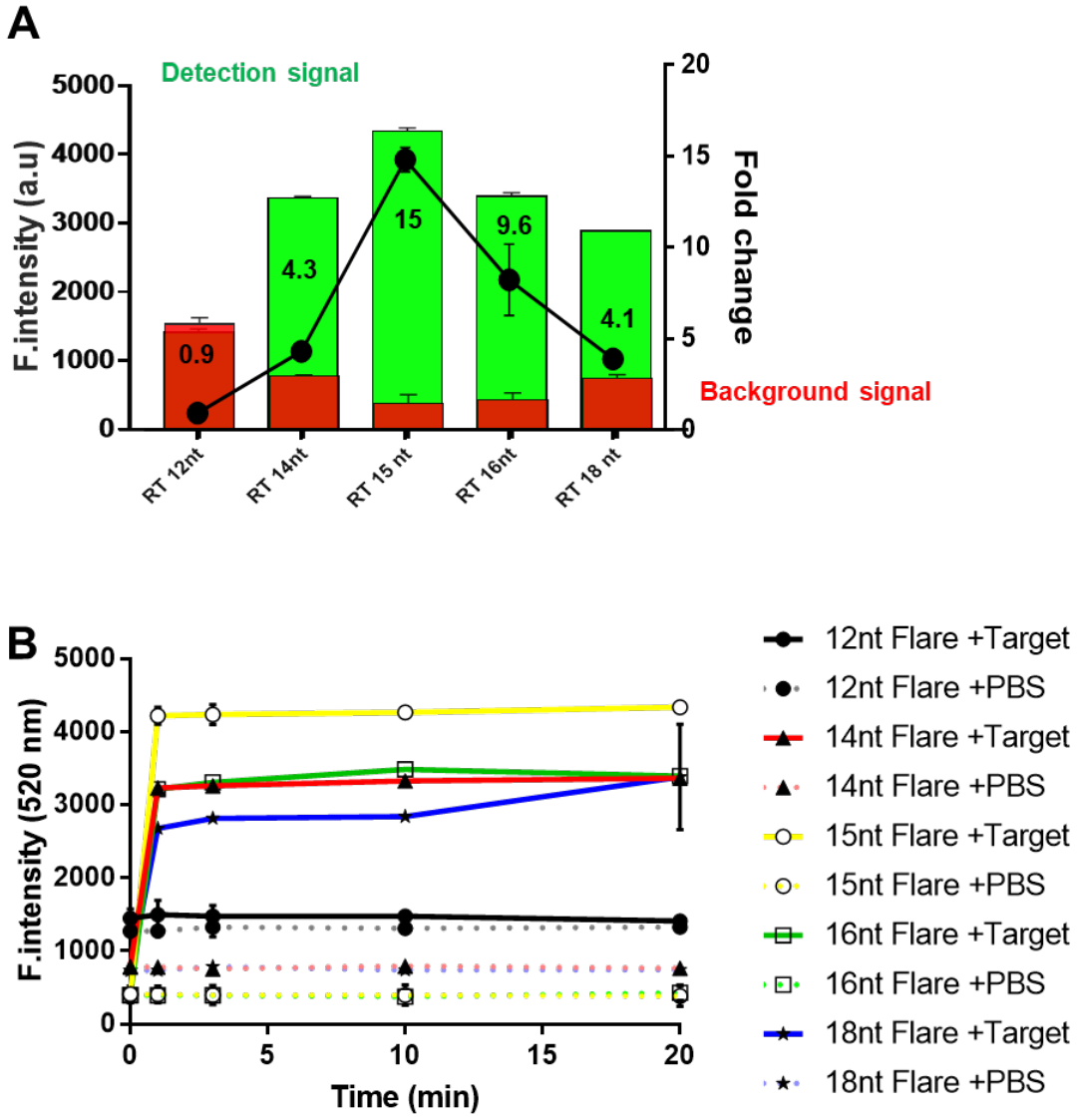

Supplementary Figure S4. Upon the addition of target sequence, the changes of fluorescence signals of FSP1-NFs that were synthesized with 12, 14, 15, 16, 18 and 20 nucleotide-long flare sequences: (A) quantification of the fluorescence signal changes; **(B)** the change of fluorescence over time (n=3, NFs concentration: O.D 0.4, Target= 2 µM, values are means ± s.d.).

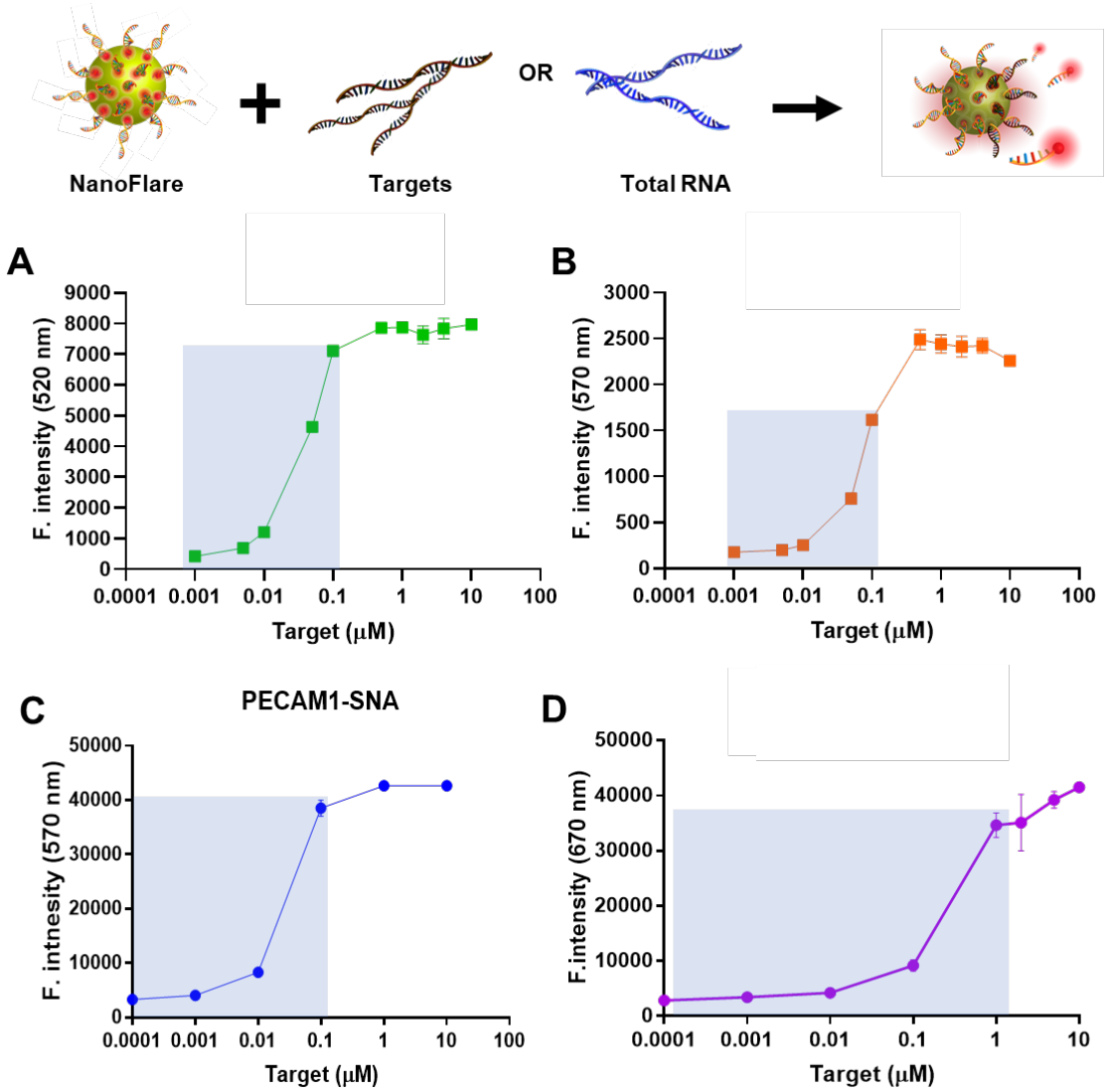

Supplementary Figure S5. Restoration of (**A**) FSP1-NFs; (**B**) KRT14-NFs; (**C**) PECAM1-NFs; (**D**) GAPDH-NFs fluorescence under different concentrations of target sequences (n=3, values are means ± s.d.).

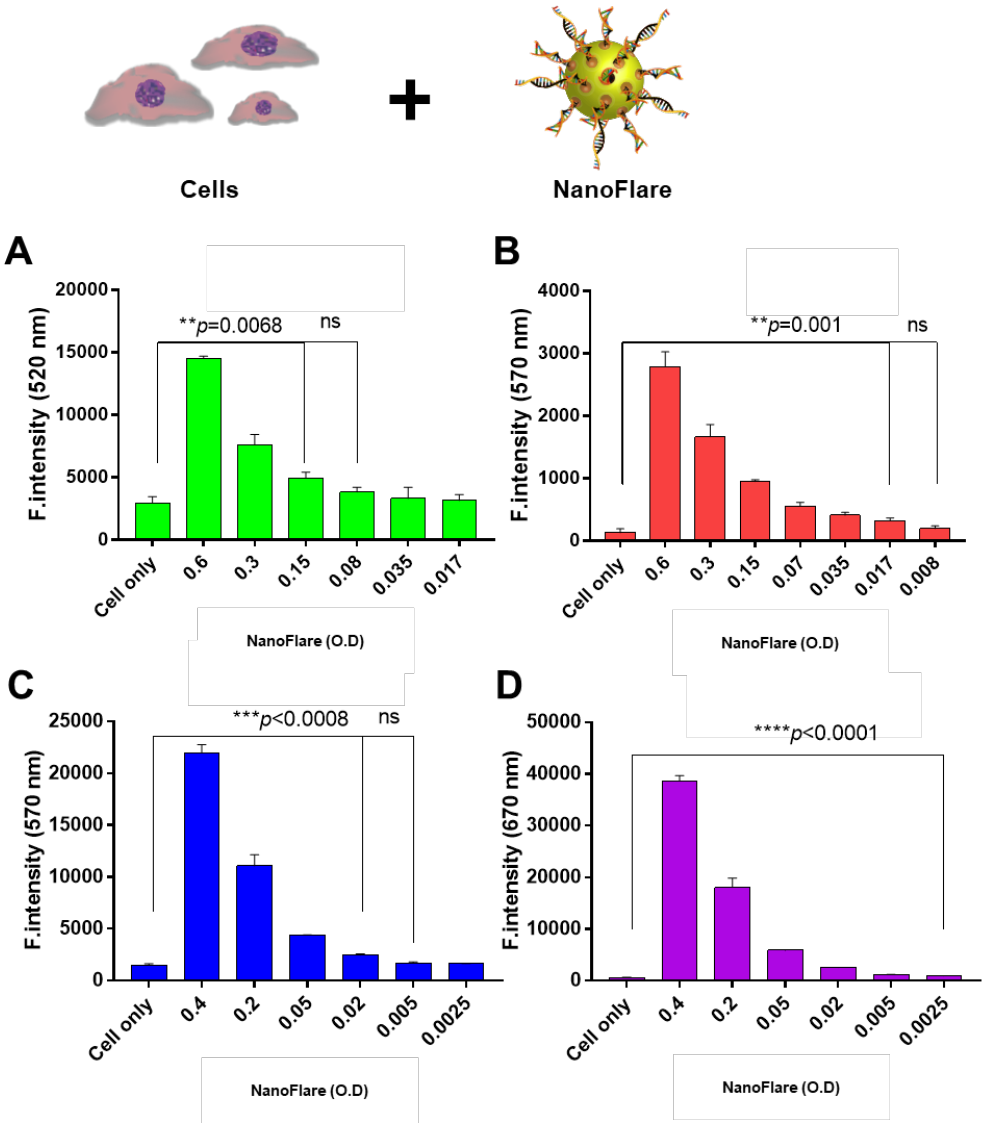

Supplementary Figure S6. Optimization of **(A)** FSP1-NFs; **(B)** KRT14-NFs; **(C)** PECAM1-NFs; **(D)** GAPDH-NFs working concentrations using cell experiments. (n=3, $5x10^4$/mL cells were labeled with NFs in 24 hrs, (**p<0.01, *** p <0.001, **** p <0.0001, and ns= not significant, n=3, values are means ± s.d.).

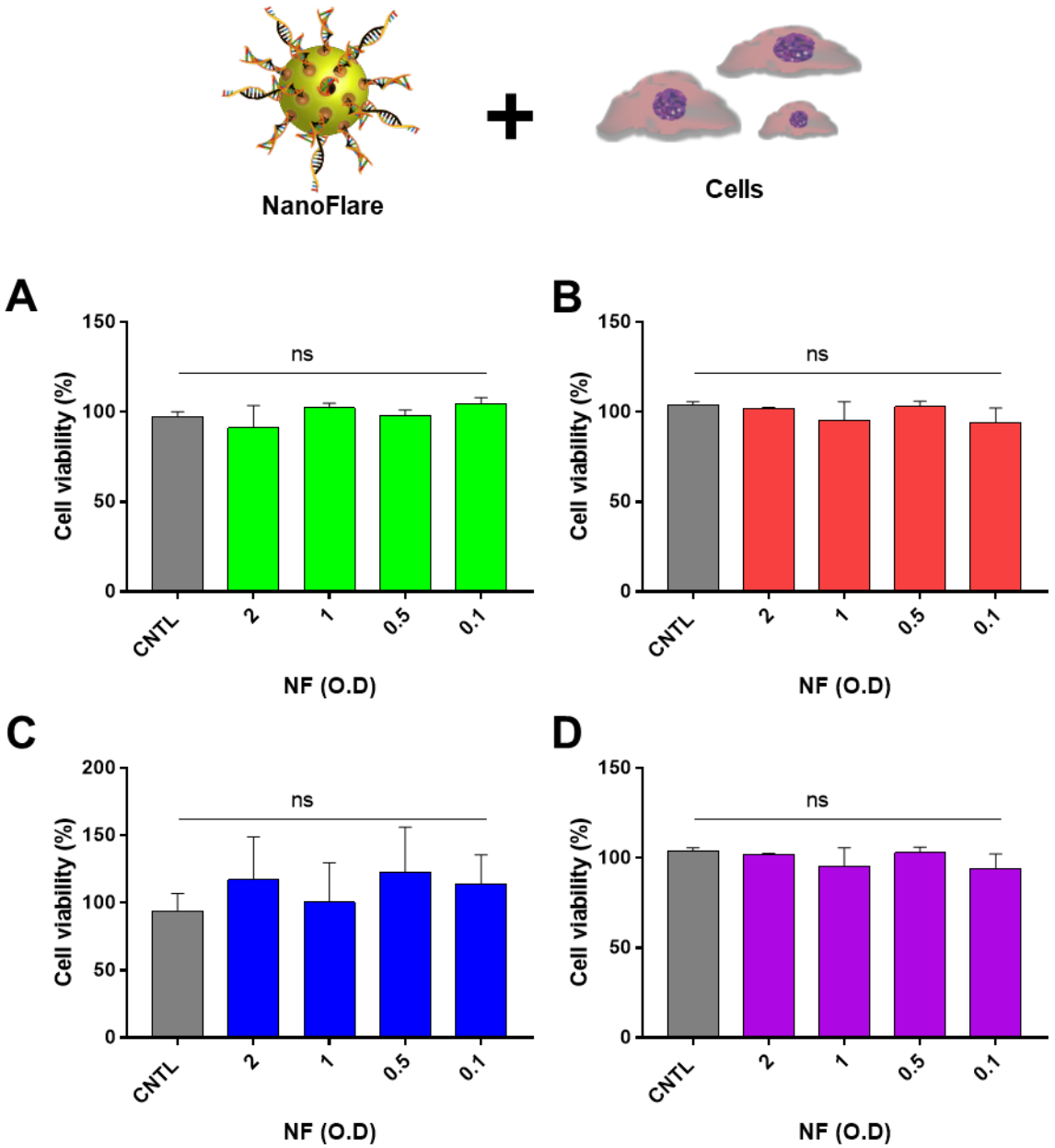

Supplementary Figure S7. Cytotoxicity study of **(A)** FSP1-NFs on NDF; **(B)** KRT14-NFs on HaCaT; **(C)** PECAM1- NFs on HUVEC; **(D)** GAPDH-NFs on HUVEC (CNTL=no treat, ns= not significant, $5x10^4$/mL cells were cultured with NFs in 24 hrs, n=3, values are means ± s.d.).

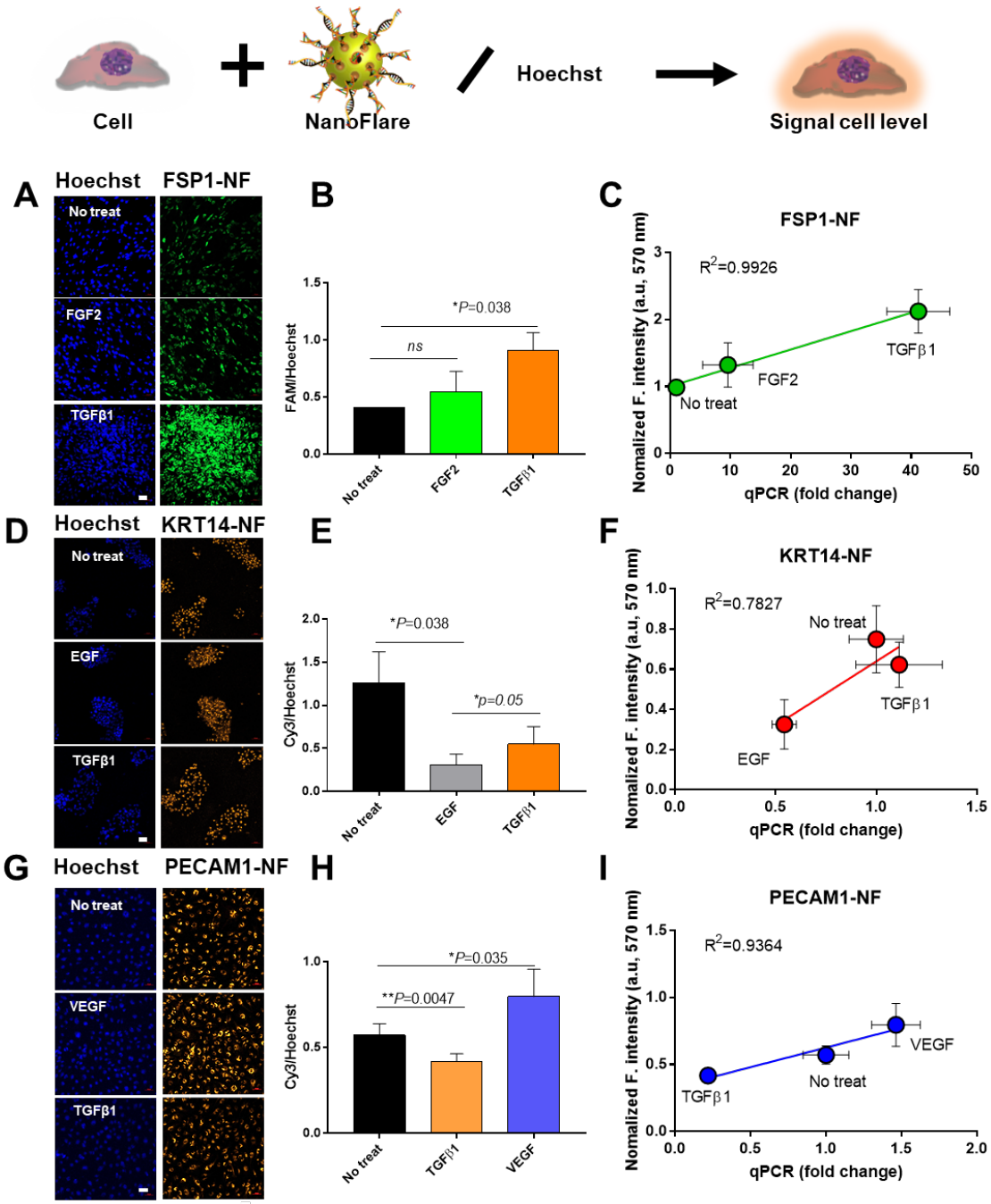

Supplementary. Figure S8. Evaluation of target gene expression in cells by NFs.(A) Fluorescence images of FSP1-NF labeled NDFs (Control: no treat, FGF2: 40 ng/mL, TGFβ1: 40 ng/mL, scale bar =50 μm); (B) Normalized FSP1-NF signal by taking Hoechst as the reference; (C) Correlation between the normalized FSP1-NF signal and qPCR results; (D) Fluorescence images of KRT14-NF labeled HaCat (Control: no treat, EGF: 40 ng/mL, TGFβ1: 40 ng/mL, scale bar =50 μm); (E) Normalized KRT14-NF signal by taking Hoechst as the reference; (F) Correlation between the normalized KRT14-NF signal and qPCR results; (G) Fluorescence images of PECAM1-NF labeled HUVEC (Control: no treat, VEGF: 40 ng/mL, TGFβ1: 40 ng/mL, scale bar =50 μm); (H) Normalized PECAM1-NF signal by taking Hoechst as the reference; (I) Correlation between the normalized PECAM1-NF signal and qPCR results (NFs=O.D 0.1 for FSP-NF, 0.0125 for KRT14-NF and PECAM1-NF, cells were starved and cultured in serum reduced media for 2 days before NF treatment, $^{**}p<0.01$, $^{***}p<0.001$, and ns= not significant, n=3, values are means ± s.d.).

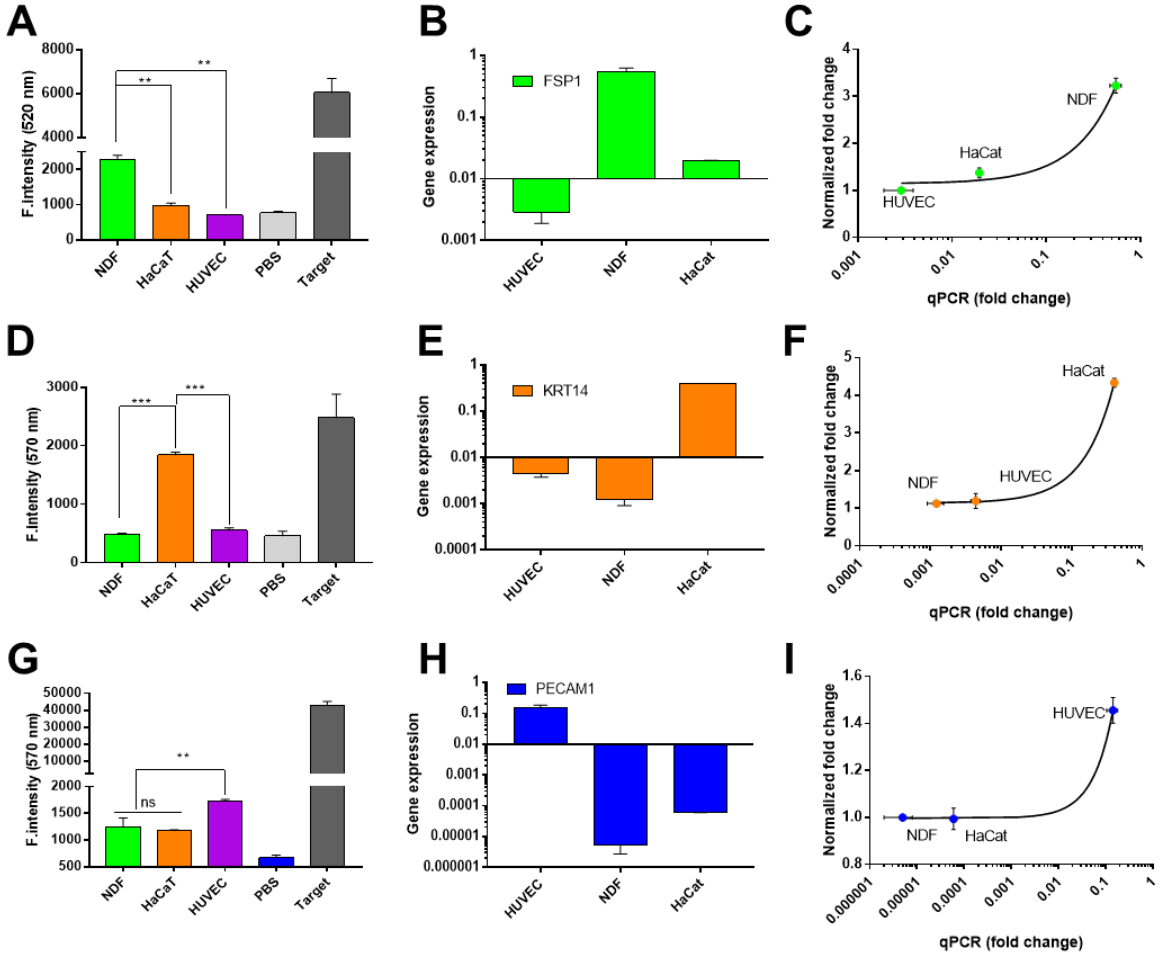

Supplementary Figure S9. **Quantification of target gene expression in cells: (A)** FSP1 expression in three types of cells evaluated by FSP1-NF (total RNA of 100 ng/µL, NF=O.D 0.4); **(B)** qPCR evaluation of FSP1 expression in cells; **(C)** Correlation between the normalized FSP1-NF signal and qPCR results; **(D)** KRT14 expression in three types of cells evaluated by KRT14-NF (total RNA of 100 ng/µL, NF=O.D 0.4); **(E)** qPCR evaluation of KRT14 expression in cells; **(F)** Correlation between the normalized KRT14-NF signal and qPCR results; **(G)** PECAM1 expression in three types of cells evaluated by PECAM1-NF (total RNA of 100 ng/µL, NF=O.D 0.4); **(H)** qPCR evaluation of PECAM1expression in cells; **(I)** Correlation between the normalized PECAM1-NF signal and qPCR results. Values are means ± s.d. (**p<0.01, *** p <0.001, and ns= not significant, n=3, values are means ± s.d.).

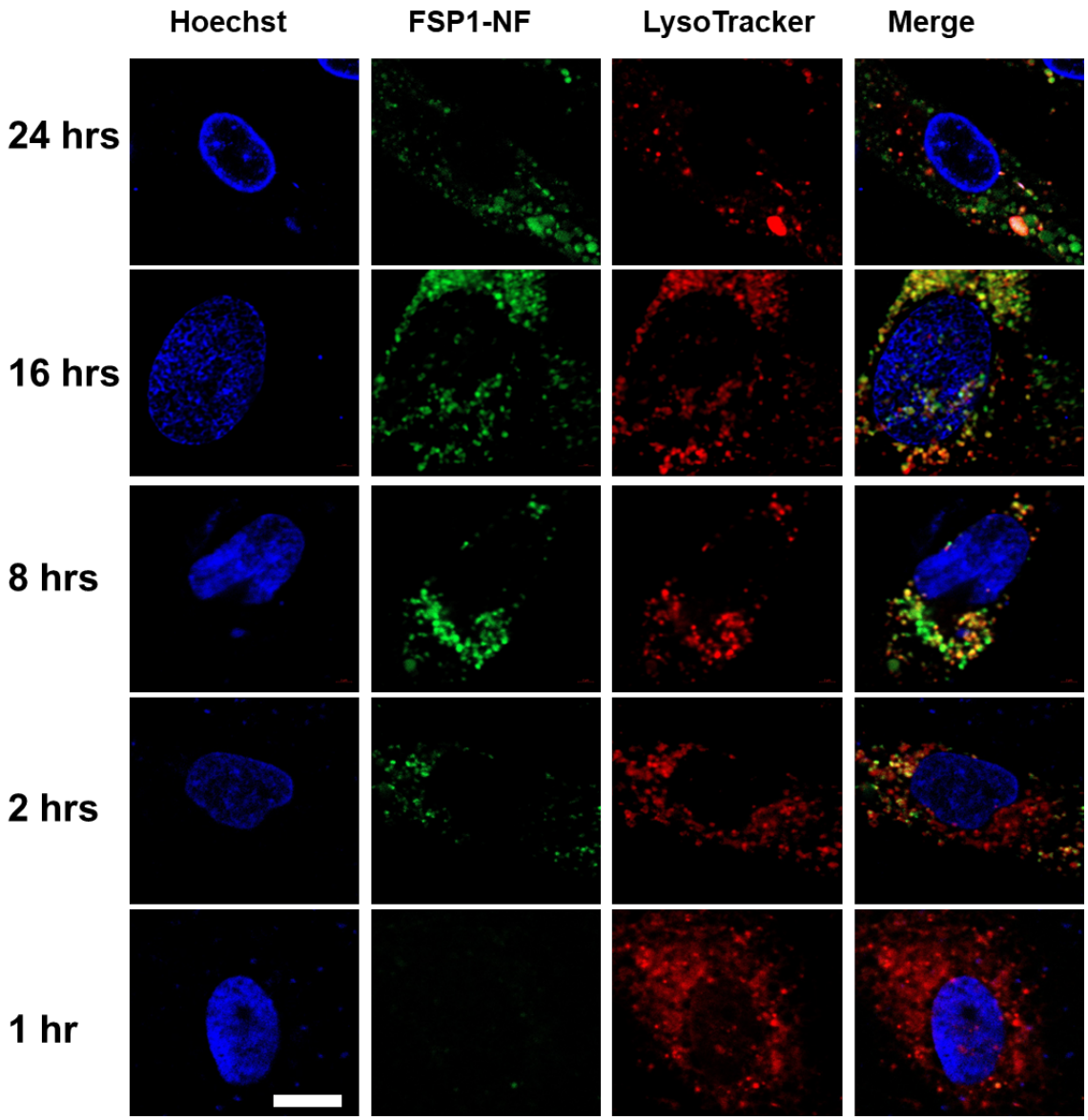

Supplementary Figure S10. Confocal fluorescence images of NDFs labeled with FSP1-NFs at different time points. Cells were pre-stained with Lysotracker. Scale bar is 20 μm, Cy3: lysotracker, Blue: Hoechst, and Green: FSP1-NFs.

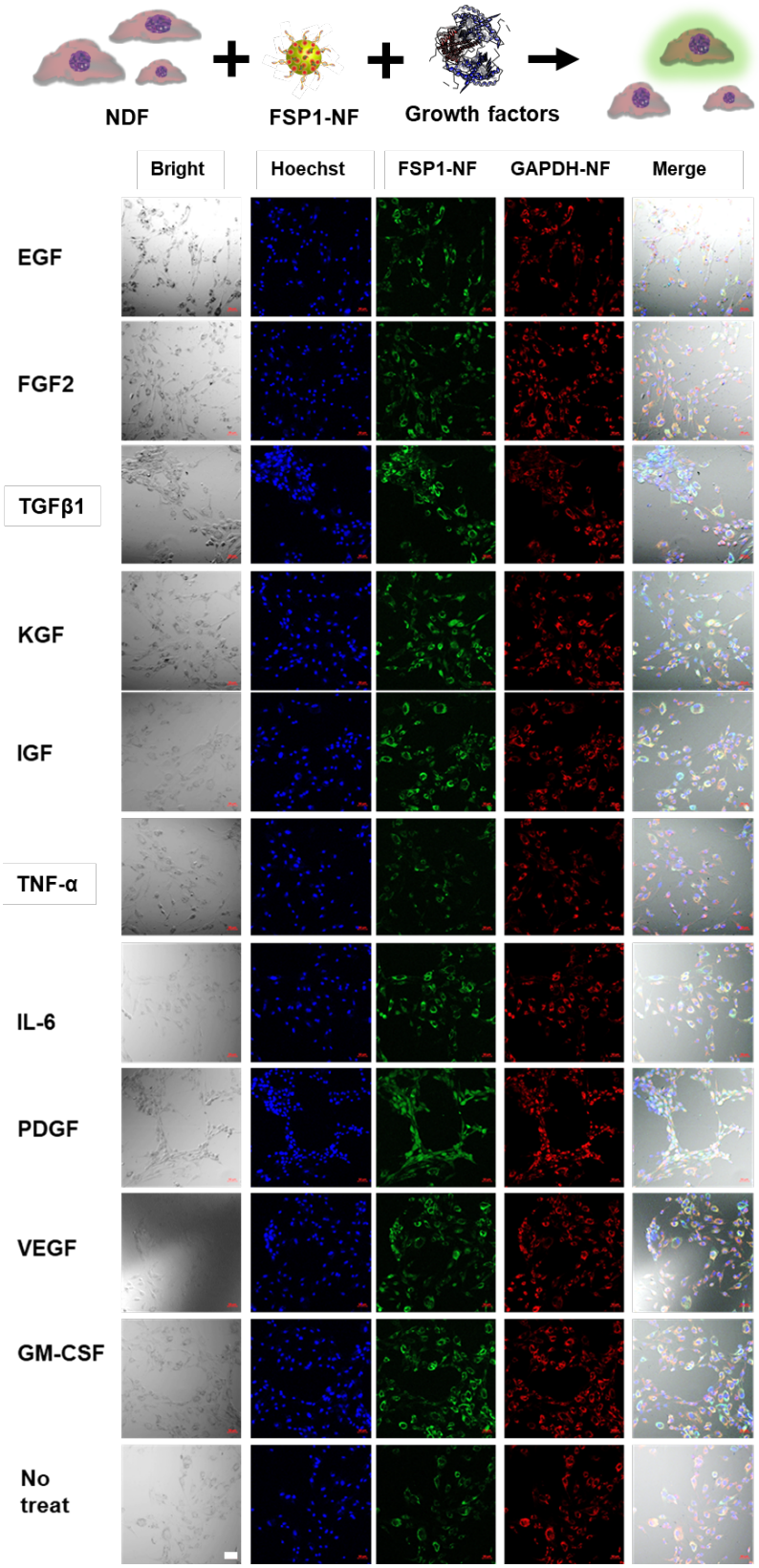

Supplementary Figure S11. Fluorescence images of NDF treated with 10 growth factors and NFs. (CNTL: no treat, EGF: 40 ng/mL, FGF2: 40 ng/mL, TGFβ1: 40 ng/mL, KGF: 40 ng/mL, IGF:40 ng/mL, TNF-α: 40 ng/mL, IL-6: 40 ng/mL, PDGF: 8 ng/mL, VEGF: 20 ng/mL, GM-CSF: 20 ng/mL) Scale bar is 50 μm. The concentrations of FSP1-NF and GAPDH-NF were O.D 0.4 and 0.0125 respectively.

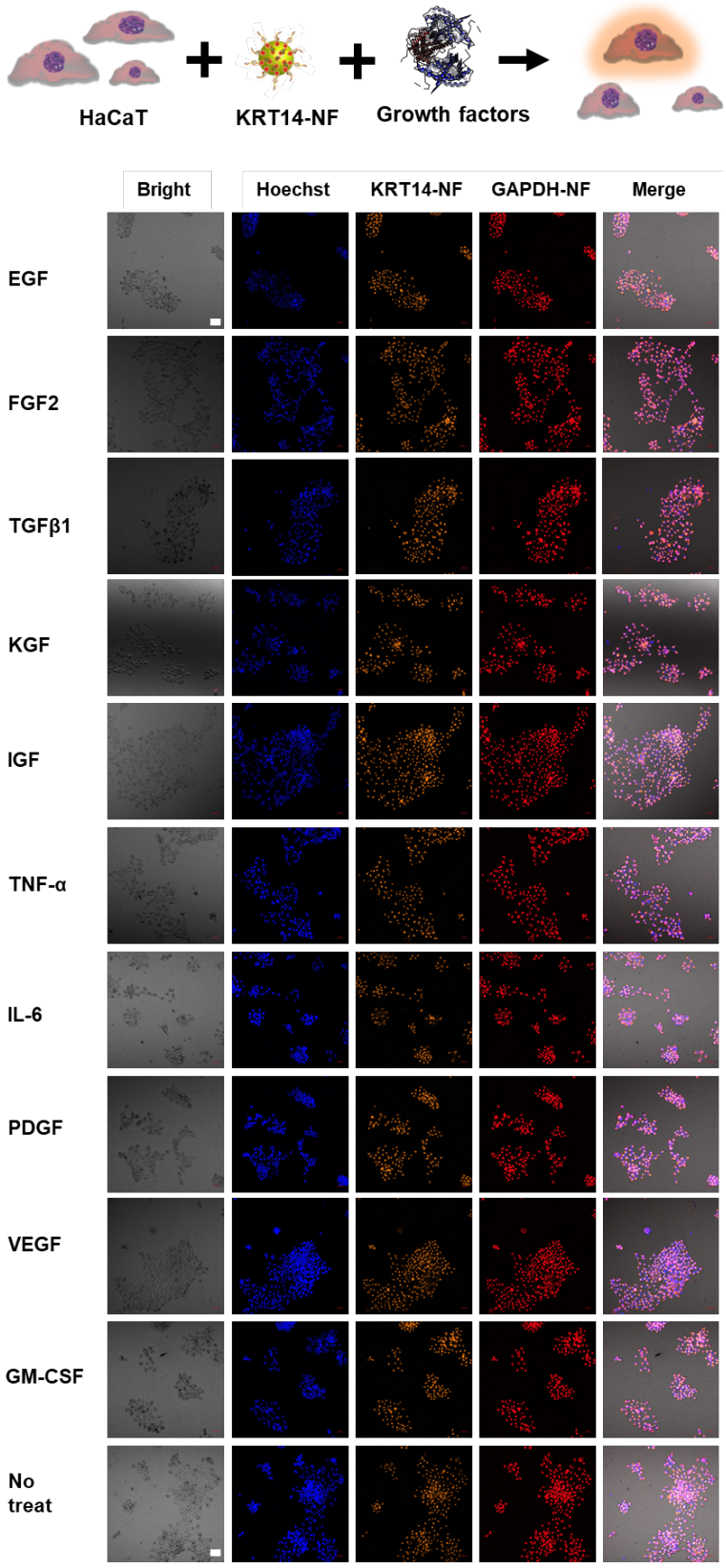

Supplementary Figure S12. Fluorescence images of HaCaT treated with 10 growth factors and NFs. (CNTL: no treat, EGF: 40 ng/mL, FGF2: 40 ng/mL, TGFβ1: 40 ng/mL, KGF: 40 ng/mL, IGF:40 ng/mL, TNF-α: 40 ng/mL, IL-6: 40 ng/mL, PDGF: 8 ng/mL, VEGF: 20 ng/mL, GM-CSF: 20 ng/mL, scale bar =50 μm, Both concentrations of KRT14-NF and GAPDH-NF were 0.0125.

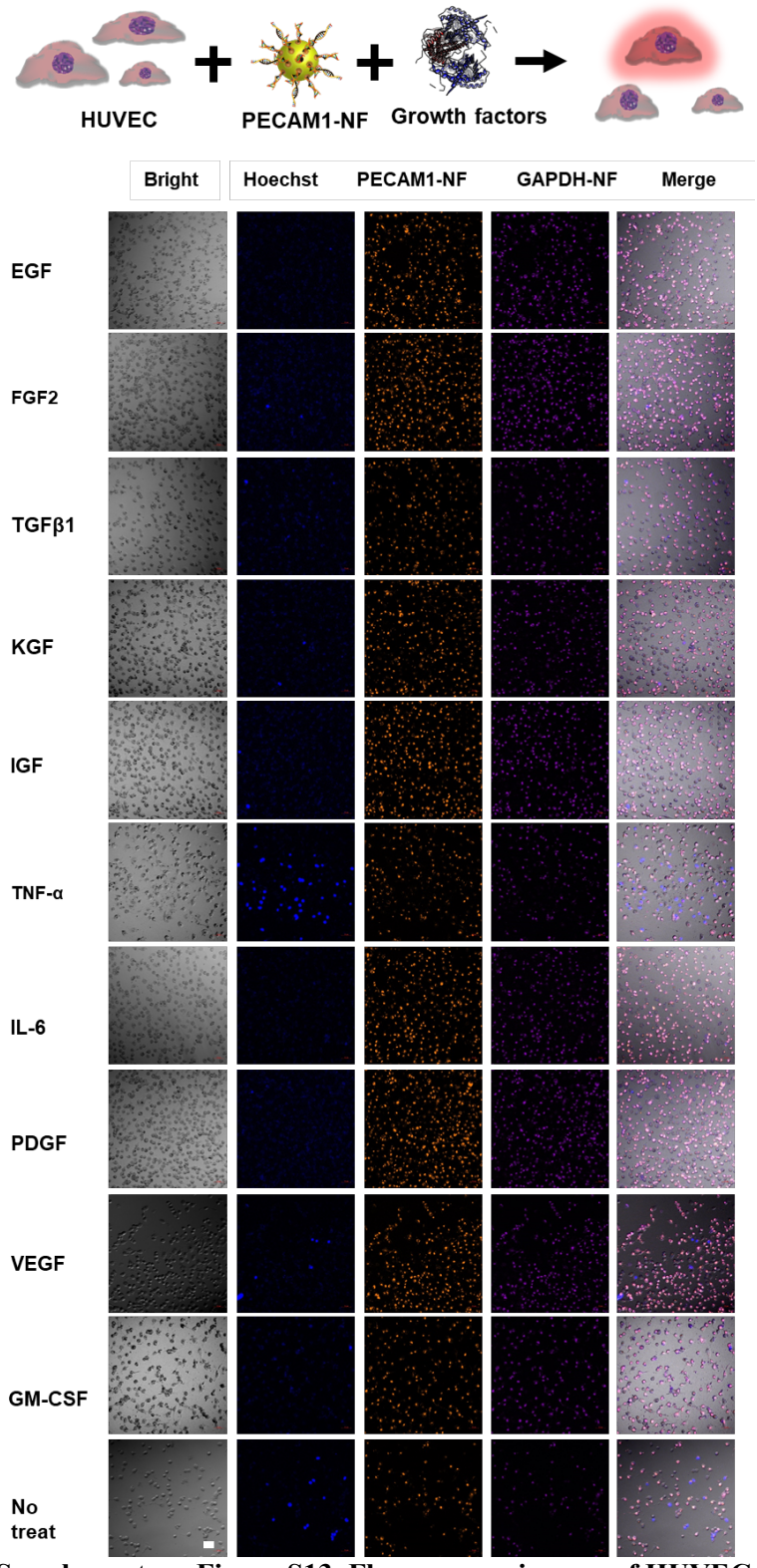

Supplementary Figure S13. Fluorescence images of HUVEC treated with 10 growth factors and NFs. (CNTL: no treat, EGF: 40 ng/mL, FGF2: 40 ng/mL, TGFβ1: 40 ng/mL, KGF: 40 ng/mL, IGF:40 ng/mL, TNF-α: 40 ng/mL, IL-6: 40 ng/mL, PDGF: 8 ng/mL, VEGF: 20 ng/mL, GM-CSF: 20 ng/mL, scale bar =50 μm, Both concentrations of PECAM1-NF and GAPDH-NF were O.D 0.0125.

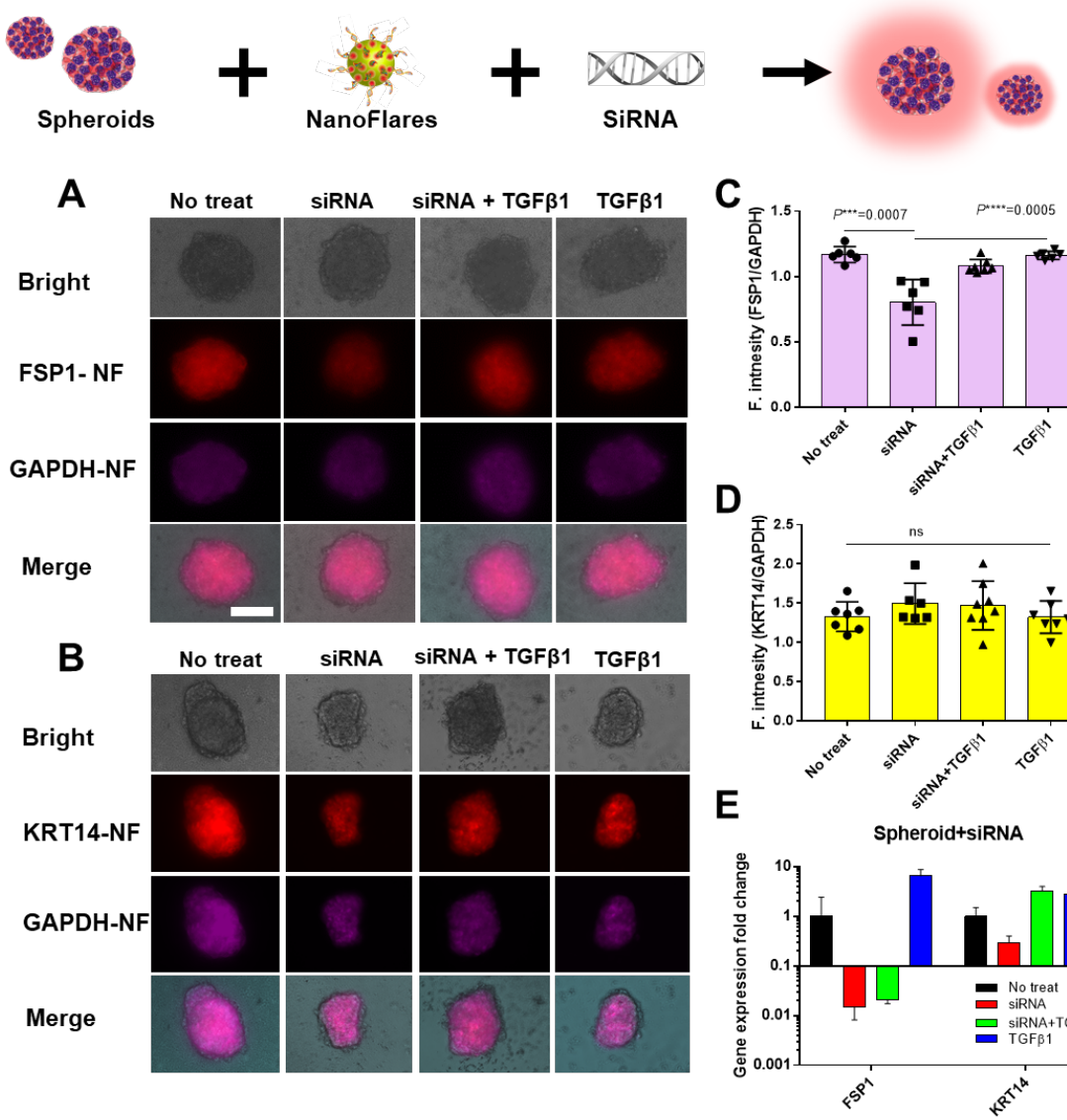

Supplementary Figure S14. Monitoring the cellular gene changes in 3D spheroid using NFs: (A) Fluorescence images of FSP1-NF labeled NDF spheroids that were pre-treated with TGFBR1 siRNA, TGFBR1 siRNAs +TGFβ1, and TGFβ1. (n=10, scale bar =100 μm); **(B)** Fluorescence images of KRT14-NF labeled HaCaT spheroids that were pre-treated with TGFBR1 siRNA, TGFBR1 siRNAs +TGFβ1, and TGFβ1 (n=10, scale bar =100 μm); **(C)** Quantification of FSP1 NF signals in **A**; **(D)** Quantification of KRT14 NF signals in B; **(E)** qPCR results of FSP1 and KRT14 expression in 3D spheroids. Values are means ± s.d. (*** p <0.001, **** p <0.0001, and ns= not significant, values are means ± s.d.).

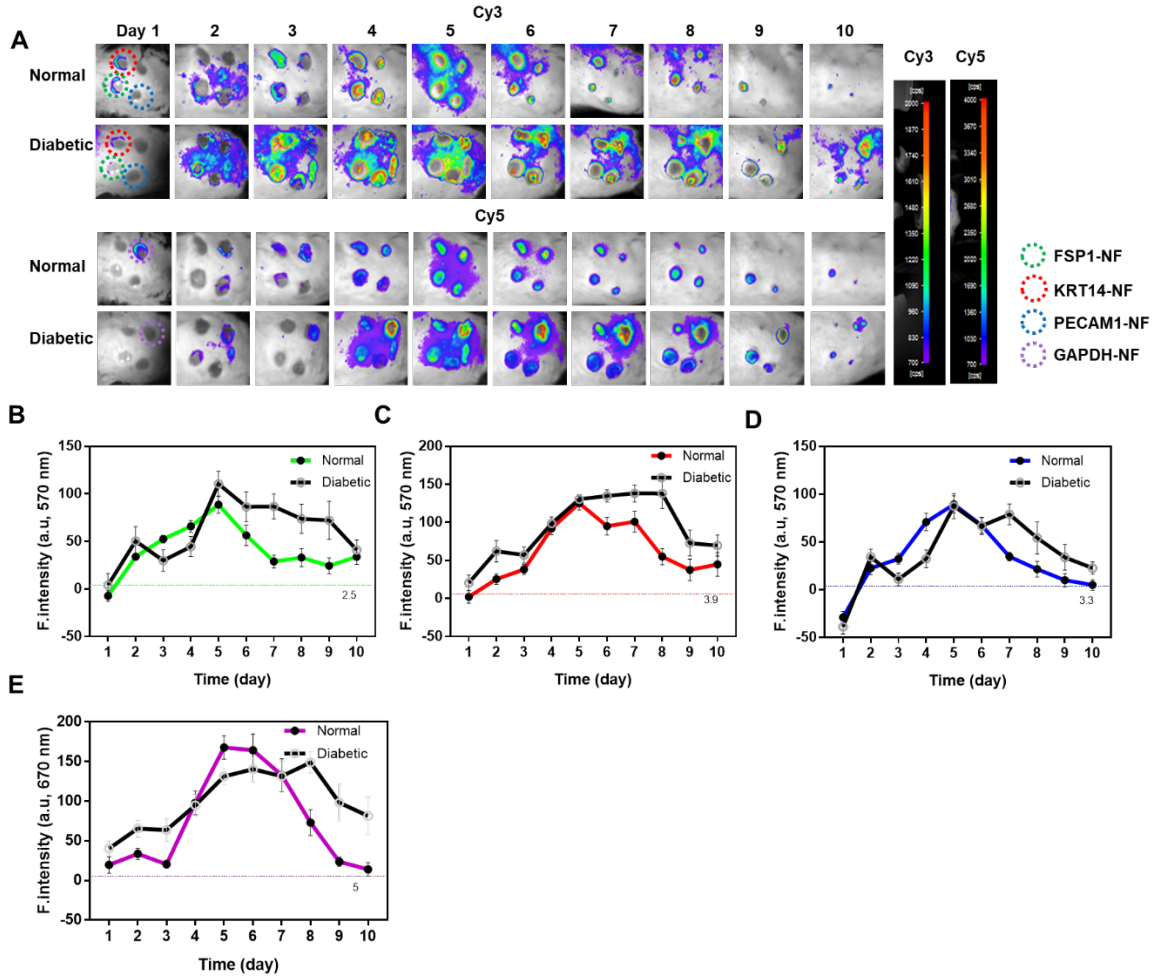

Supplementary Figure S15. Tracking wound healing process using NFs on normal and diabetic wound healing models: (A) IVIS imaging of mice post NFs application (FSP1-NF treated wound: green circles; KRT14-NF treated wound: red circle; PECAM1-NF treated wound: blue circles; GAPDH-NF treated wound: purple circle; Mean fluorescence intensity of **(B)** FSP1-NF, **(C)** KRT14-NF, **(D)** PECAM1-NF, **(E)** GAPDH-NF from both wound groups (n = 11, duplicate, mean with SEM).

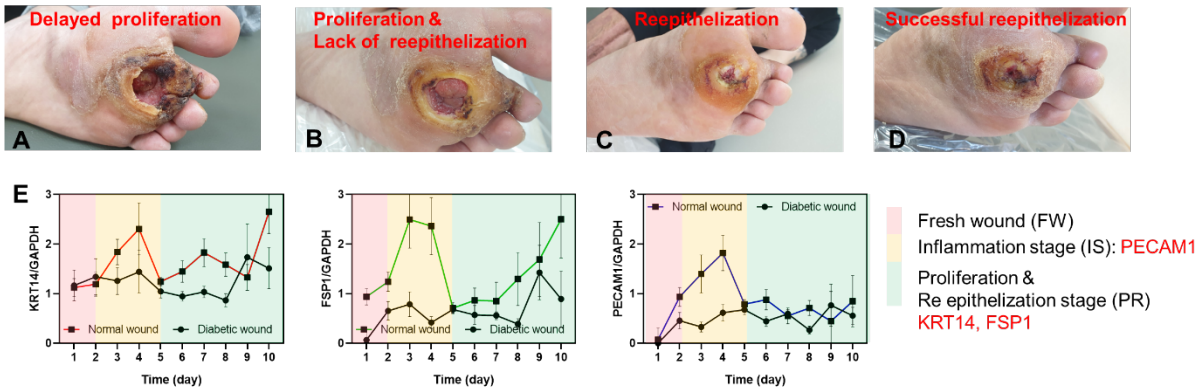

F

	KRT14 NF		FSP1 NF		PECAM1 NF	
	Normal	Diabetic	Normal	Diabetic	Normal	Diabetic
Fresh Wound	1	1	0-1	1	<1	<1
Inflammation stage	1-2.5	0-1	1-3	0-1	**1-2**	**<1**
Proliferation & Reepithelization stage	**1-3**	**1-1.5**	**1-3**	**1-1.5**	<1	<1

Supplementary Figure S16. A wound healing algorithm for patients with diabetic foot ulcer: (A) Delayed proliferation stage; **(B)** Proliferative but lack of epithelization stage; **(C)** Starting reepithelization; **(D)** Successful reepithelization; **(E)** Evaluation of target gene expression by NFs on the normal and diabetic groups (target gene/GAPDH) from Figure 5; **(F)** Analyzed wound healing index based on NF's signal from E.